ACTA IMEKO
ISSN: 2221-870X
June 2025, Volume 14, Number 2, 1 - 11

Shoot architectural analysis for olive cultivar characterization: an automatic internode measurement procedure

Alessandro Annessi[1], Andrea Berdini[2], Francesco Belluccini[1], Matteo Zucchini[1], Veronica Giorgi[1], Enrico Maria Lodolini[1], Milena Martarelli[2], Paolo Castellini[2], Davide Neri[1]

[1] *Department of Agricultural, Food and Environmental Sciences, Università Politecnica delle Marche, Ancona, Italy*
[2] *Department of Industrial Engineering and Mathematical Sciences, Università Politecnica delle Marche, Ancona, Italy*

ABSTRACT
Tree architecture, defined as the arrangement in space of the elements above the ground, is closely related to the biological and physiological processes of the tree. In particular, the quantitative study of the branch consists of classifying branches into orders, estimating lengths, insertion angles, diameters and volumes. In the case of the olive tree (*Olea europaea* L.), the knowledge of its architecture is important to determine which varieties are suitable for high-density planting systems and to guide canopy pruning, which allow simplification of field management and reduction of costs. Up to date, measurements are mainly done manually, using measuring tape and caliper, with high time expense and operator-related uncertainty. In this study, the analysis is extended to the three-dimensional case using photogrammetry. Next, the point cloud is processed using a modified version of the open-source code TreeQSM (version 2.4.1). Moreover, a new methodology, based on photogrammetry and branch segmentation using TreeQSM, is proposed to measure not only average branch diameter, but also node diameter and internodal distance along the principal axis of the twig point cloud. The main characteristics of the principal axis of the twig are obtained to prove the validity of the proposed method. The node average diameter is 2.94 mm with a standard deviation of 1.20 mm while the average internode is 14.38 mm with a standard deviation of 7.78 mm.

Section: RESEARCH PAPER

Keywords: Photogrammetry; dimensional measurements; internode; branch segmentation; tree architecture

Citation: A. Annessi, A. Berdini, F. Belluccini, M. Zucchini, V. Giorgi, E. M. Lodolini, M. Martarelli, P. Castellini, D. Neri, Shoot architectural analysis for olive cultivar characterization: an automatic internode measurement procedure, Acta IMEKO, vol. 14 (2025) no. 2, pp. 1-11. DOI: 10.21014/actaimeko.v14i2.2063

Section Editor: Andrea Scorza, University Roma Tre, Italy

Received January 28, 2025; **In final form** June 17, 2025; **Published** June 2025

Funding: This work was supported by TeneRa of the operational group RiTA (ID 59750), "Valorization of genetic resources and introduction of innovative techniques for Ascolana tenera production" founded by PSR Marche 2014-2020 (16.1).

Corresponding author: Alessandro Annessi, e-mail: a.annessi@staff.univpm.it

1. INTRODUCTION

Tree architecture, defined as the arrangement in space of the elements above the ground, is closely related to the biological and physiological processes of the tree itself [1]. In particular, the quantitative study of the branch, as a growing unit in a growth cycle, consists of classifying branches into orders, estimating lengths, insertion angles, diameters and volumes. In the case of the olive tree (Olea europaea L.), knowing its architecture is important to determine which varieties have compact internodes and, therefore, if they are more suitable for high-density planting systems, which allow simplification of field management and reduction of costs [2]. In addition, the quantitative branch model is useful for quantifying biomass availability [3] even for the energetic valorisation of the pruning residues [4]. The latter considerations are completely consistent with the Precision Agriculture (PA) framework, which allows an enhancement in terms of efficiency and profitability of the farm [5] also through the use of sensor networks [6].

The required characteristics for an olive variety to be suitable for high-density plantings are compact tree growth, high branching density and regular fruit production [7]. These characteristics are dependent on the number of nodes per stem unit and thus on the length of the internode (i.e., the distance that occurs between two consecutive nodes). The node is the point of insertion of the leaves and the meristems that can

originate shoots or inflorescences along the main axis of a shoot. In general, this corresponds to an enlargement of the shoot that remains visible in the branch in the subsequent years even after, for example, leaves have fallen, or buds have not developed [8]. For the reasons previously listed, reliable estimation of the geometric characteristics of the shoot and, specifically, of the internode is of particular interest in the agricultural sector of olive growing.

To date, these assessments are done manually, using measuring tape and caliper, with high time expenditure and operator-related uncertainty. Therefore, the scientific community is seeking innovative and reliable methods for estimating the geometric characteristics of branches in less time and cost. Carella et al. used a single camera setup and adapted image analysis techniques, already used for root analysis, to branch analysis of defoliated olive branches to evaluate branch and shoot size and architecture in a two-year-old olive tree bearing branches. This approach made the process more automatic, standardized and repeatable but the analysis is carried only on images, retrieving 2-d geometric characteristic [9].

To overcome this limitation, methodologies for measuring 3-d tree point clouds based on non-contact systems, such as Terrestrial Laser Scanning (TLS), were used for tree architecture estimation. TLS technique uses a Light Detection and Ranging (LiDAR) device to obtain a 3-d scan of the target area. Lin et al. developed a TLS network for macroscale analysis of the global 3D structure of tall trees [10]. Yang et al. presented a new approach to tree architectural properties estimation using TLS data [11]. Åkerblom et al. exploited tree Quantitative Structural Models (QSM) to extract geometrical features for species recognition. QSM are hierarchical geometric primitive models that accurately approximate the arrangement of branches, geometry, and volume of the trees [12].

LiDAR and Structure-from-Motion (SfM) techniques are extensively used in a wide range of applications spanning from archaeological site evaluation [13], [14] and environmental assessment [15], [16] to the engineering field [17], [18]. LiDAR techniques are remarkably more expensive but usually provide a higher spatial resolution if compared to SfM techniques. On the other hand, SfM techniques are easy to use, since they do not need specific instrumentation, and cost effective but offer a lower spatial resolution.

In this work, we tackle the problem of branch architecture geometric characteristics estimation for medium branches and small bearing shoots for the purpose of species and variety classification. A three-dimensional analysis was conducted using a photogrammetric approach taking advantage of a standard reflex digital camera. The point cloud obtained from the scan was processed with the open-source TreeQSM algorithm (version 2.4.1) [19]-[21] for the estimation of geometric features and branch segmentation of the tree. Average branch diameter and branch length, divided by branching order, are the standard outcome from the algorithm to estimate the total volume of timber in the case of tall trees. In the case of species and variety classification, further geometrical features need to be considered such as node diameter and internodal distance, which is referred as internode. Therefore, a new methodology is then proposed to measure the proper average branch diameter excluding nodes from the calculation and retrieving the node diameter and the internode. Special attention is given to estimating the uncertainty associated with the measurement of branch diameters and lengths, which affect the calculation of internodal distances. For this purpose, a sensitivity analysis to varying algorithm input parameters, measurement noise and geometry was conducted by Monte Carlo technique.

The paper is structured as follows. Section 2 describes the measurement setup and the image acquisition process for the point cloud reconstruction. Section 3 explains the measurement methodology used in the present work and the issue that arose concerning diameter measurement. In Section 4, a sensitivity analysis is carried out to estimate the uncertainty on diameters and lengths. The proposed algorithm is applied to the reconstructed point cloud in Section 5 estimating node diameters and internodes. Finally, findings and future challenges are summarized in Section 6.

2. POINT CLOUD OF AN OLIVE TREE BRANCH

In order to demonstrate the reliability of the proposed methodology for measuring the diameters and internode distances of olive tree branches, a terminal branch with defoliated sylleptic shoots was used as a case study, as shown in Figure 1. The schematic of the setup for image acquisition is shown in Figure 2a while its realisation is shown in Figure 2b. This consists of a white cardboard box, to obtain a uniform background, a Nikon D7200 camera equipped with a Nikon AF-S 60mm f/2.8G ED Micro and a halogen illumination system, consisting of two 500 W halogen lamps positioned symmetrically and oriented at 40° angle with respect to the camera-branch plane. Experimental setup components along with the related specifications are listed in Table 1.

The branch is mounted on a graduated rotating base with a customized marker strip glued on it, as shown in Figure 2c. This consists of a black strip with white alphabetic letters on it, having known dimensions. The high contrast of the letters contours in the marker strip allows to obtain a better alignment of the images in the SfM software, as the object has no repeatable, highly contrasted patterns. Moreover, the black-and-white lettering strip is used to scale the point cloud in engineering units. A total of 180 images of the branch or its parts were acquired, with

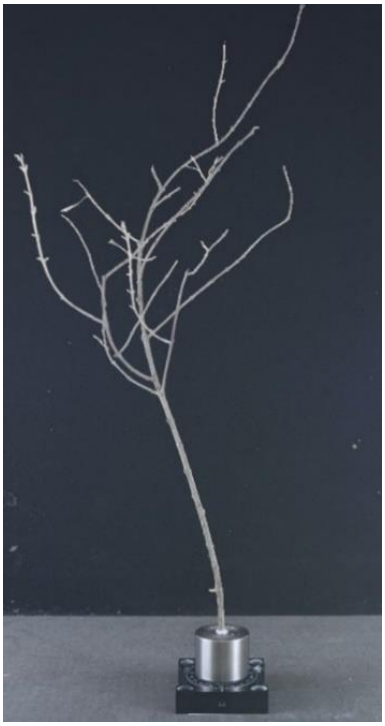

Figure 1. Defoliated olive tree branch chosen for the test.

Table 1. List of setup components and specifications.

	Component	Information	Specifications
1.	Camera	Nikon D7200	• Sensor size APS-C (23.5 x 15.6 mm) • 24.2MP CMOS sensor with no optical low-pass filter • ISO 100-25600 • 1/8000 s maximum shutter speed • Buffer depth: 18 Raw, 100 JPEG
2.	Lens	Nikon AF-S 60mm f/2.8G ED Micro	• Focal length 60mm • Maximum aperture f/2.8 • Minimum aperture f/32 • Closest focusing distance 0.185 m
3.	Lighting	Halogen lamps	• Power 500 W

Table 2. Camera intrinsic parameters retrieved from calibration process with chessboard.

	Value	Description
f	15583.7881	Focal length measured in pixels (in pixels)
$k1$	0.0109437	Radial distortion coefficients (dimensionless)
$k2$	-1.70007	
$k3$	47.3682	
$k4$	2.75392	
cx	-23.5719	Principal point coordinates (in pixels)
cy	5.96687	
$p1$	-0.000140832	Radial distortion coefficients (dimensionless)
$p2$	-0.000504439	
$b1$	3.62832	Affinity and non-orthogonality (skew) coefficients (in pixels)
$b2$	1.50705	

different angular resolution, for the point cloud reconstruction. The images of the entire ramification taken are 72, considering an angular step of 5° for an entire angle lap. An example image is shown in Figure 3a. On the other hand, close- up images of the lower, middle and upper sections are acquired with an angular resolution of 10°, obtaining 36 images for each section. The latter images are needed to reach an optimal alignment and reconstruction. Having a fixed focal length lens available, images were acquired at different distances to capture the whole shooting branch or a particular field. Moreover, the distance of the camera from the sample is not mandatory because SfM software is based on feature alignment between images. For each photo acquired, the sample is rotated by hand, checking the rotation visually using the angular scale present on the rotating base. Camera calibration is done using a chessboard following the guidelines from Agisoft Metashape and retrieving camera intrinsic parameters, which are listed in Table 2.

The images were processed in Agisoft Metashape software. Initially, images are masked to remove the uniform background, which was separately acquired. Afterwards, a sparse point cloud is obtained using 60000 key point maximum and 6000 tie point maximum from the alignment shown in Figure 3b. Next, a high-resolution dense point cloud having 5379553 points is retrieved. Lastly, the latter is scaled using marker points selected on the customized strip around the twig rotating base. A total of 15 marker points distributed along the whole angle are considered in the scaling process to define scale bars having known length equal to letters dimensions. An example of the marker points used is shown in Figure 3c. Finally, the scaled point cloud is

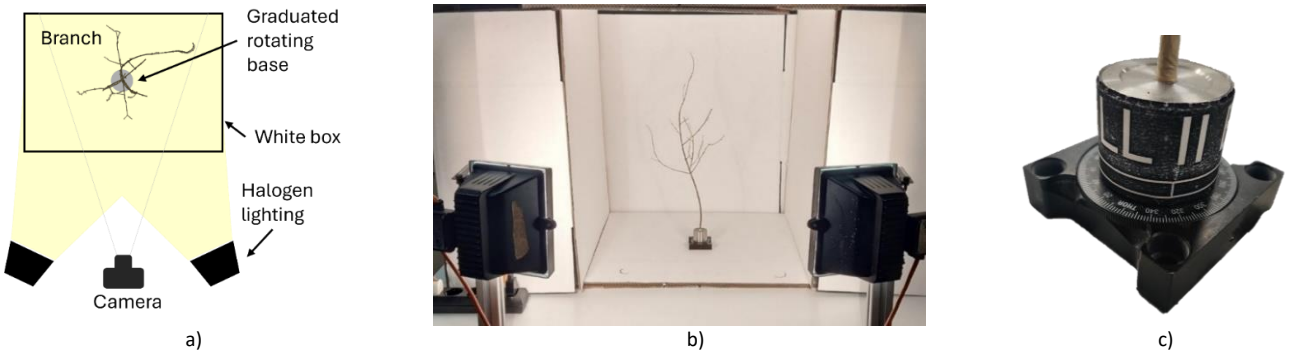

Figure 2. a) Schematic representation of the setup. b) Experimental setup in place: white box with the branch inside and halogen illumination. c) Graduated rotating base with customized marker used for reference.

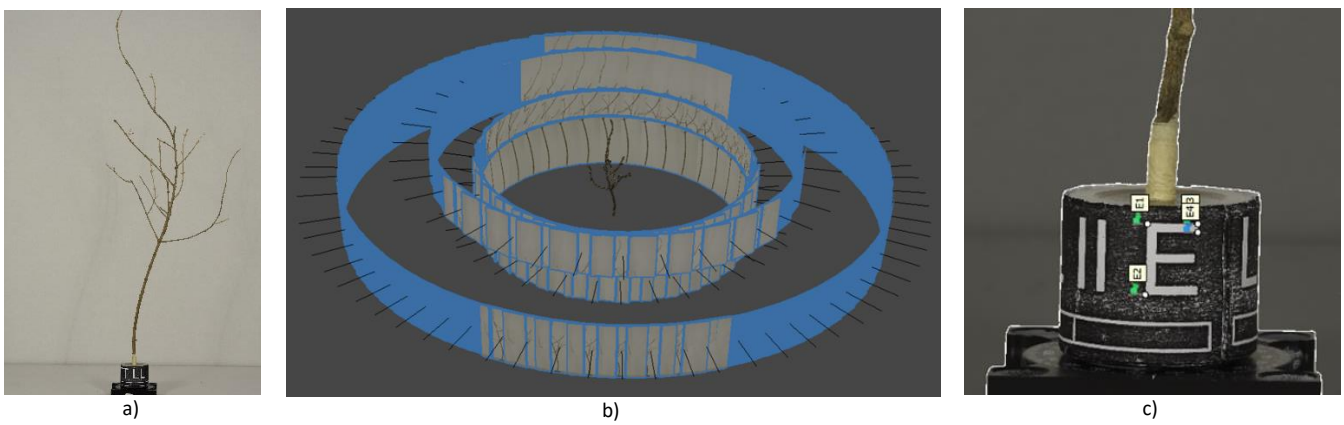

Figure 3. a) Example of an acquired image of the entire ramification. b) Image alignment using Metashape with data of the full branch with the addition of close-up images. c) Close-up of the strip marker with example marker points used to scale the point cloud.

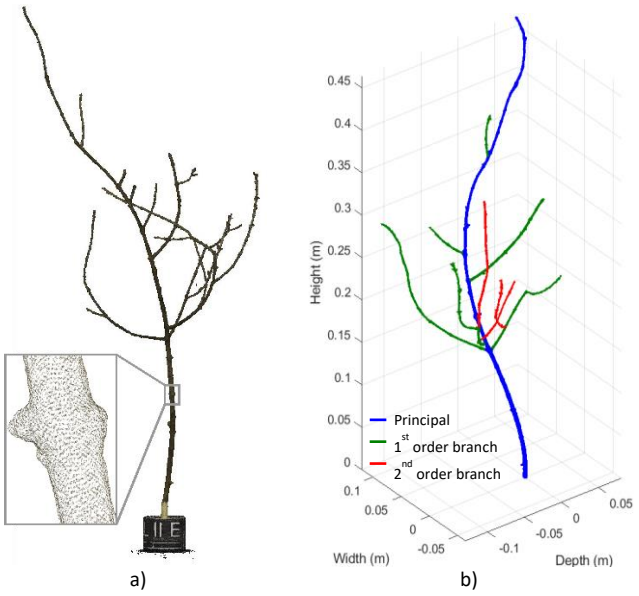

Figure 4. a) Point cloud with detail. b) Branch segmentation with TreeQSM algorithm.

shown in Figure 4a and TreeQSM algorithm is applied for geometrical model reconstruction. The TreeQSM algorithm consists of the following main steps [20]:

1. Filtering of noise present in the point cloud
2. Definition of cover sets
3. Determination of tree components
4. Segmentation in orders
5. Cylinder fitting
6. Refinement of the complete cylinder model
7. Tree geometric characteristics retrieval.

Therefore, it is possible to derive a full model of the branch architecture and obtain the segmentation into orders, which are depicted by different colours in Figure 4b. Finally, the measurements of the mean diameters ϕ and lengths l of each branch order are obtained.

The density of the point cloud is a crucial parameter for obtaining a good structural model of the branching. The minimum density value available in the literature for tall trees is 2.25 points/cm² [21]. In our case, the image acquisition is carried out on a dedicated measurement setup and the surface density of the point cloud is estimated by counting the number of points of neighbours N inside a sphere of radius R spanning the whole point cloud volume. Therefore, the surface density is given as a distribution with relative mean and standard deviation. The average surface density is 36278 points/cm² with a corresponding standard deviation equal to 7856 points/cm², considering a radius R equal to 3.5 mm, chosen accordingly to average diameter retrieved by manual measurements. The resulting value is far above the reference found in literature due to the small size of the branch, if compared to tall trees, and the high number of images acquired for the point cloud reconstruction.

3. METHODOLOGY FOR DIAMETER MEASUREMENT AND INTERNODE ESTIMATION

Figure 5a shows a section of the branch and its segmentation by TreeQSM using cylindrical elements to approximate the branch. To estimate the average diameter ϕ_n of the branch, the software considers the diameter of all cylinders identified in the segmentation, including those of the nodes (highlighted in red in Figure 5a). As a result, the average diameter ϕ_n is overestimated with respect to the true value due to the presence of nodes, which are considered as outliers, with diameters greater than the one of the branches. Figure 5b shows the estimates of the diameters for 4 different branches calculated by means of TreeQSM and measured experimentally with a centesimal caliper, considering or not the nodes. The diameter average and standard deviations are derived from 20 measurement for each case. The error bars are given as standard deviations with a coverage factor equal to 2. The diameter measured manually by averaging several measurements including the nodes is compatible with the value estimated by TreeQSM algorithm. When diameters are manually measured, values in the proximity of nodes can be excluded from the computation of the average. With this consideration, the average diameter is significantly smaller than the one estimated by TreeQSM. In order to solve this problem, a methodology is proposed that allows the automatic identification of nodes by considering the cylinder diameters corresponding to the nodes as outliers. By calculating the average diameter of the cylinders excluding the outliers, it will be possible to estimate the average diameter of the branches of the various orders with greater accuracy. Furthermore, this procedure, based on the identification of the nodes as outliers, makes it possible to determine their position along the branch, and thus to estimate the distance between the nodes, also known as the internode, as shown in Figure 5c.

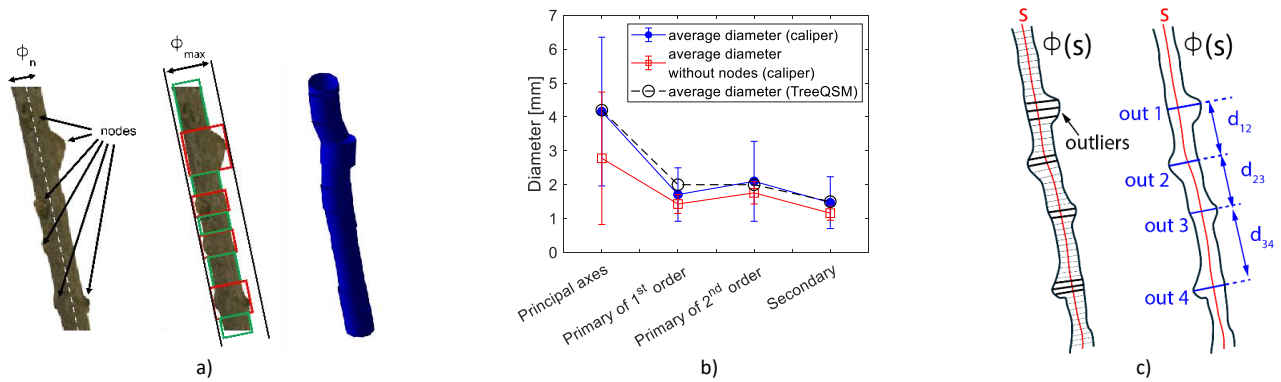

Figure 5. (a) Branch segmentation by cylinders with TreeQSM, red rectangles represent nodes while green rectangles represent branches. (b) Trend of average diameters of different orders measured manually by including and excluding node diameters and estimated by TreeQSM. (c) Identification of outliers and internode estimation.

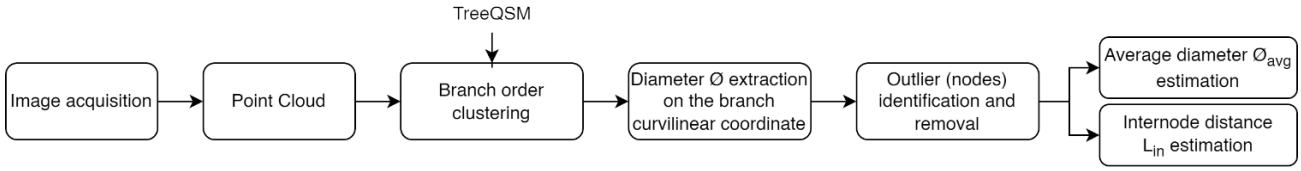

Figure 6. Flowchart of the methodology for automatic node identification and diameter measurement.

The flowchart of the procedure is shown in Figure 6. Once the images are acquired and the scaled point cloud are obtained. The segmentation is performed by labelling the branches into different order and position. Next, the diameter is evaluated along the curvilinear abscissa of the branch, passing through the axes of the identified cylinders, as shown in Figure 5c. At this point, the branch diameters relative to the nodes are identified based on continuity with adjacent diameters and excluded as outliers in the calculation of the mean diameter. The envelope function is used to smooth the diameter data along the branch curvilinear axis. The resulting diameters are considered as the starting point to identify nodes, through a threshold, as abrupt deviations from it. The positions of the outliers (i.e. nodes) along the curvilinear abscissa are then used to estimate the internodes.

4. SENSITIVITY ANALYSIS AND UNCERTAINTY ESTIMATION

In order to obtain meaningful measurements, it is necessary to identify the optimal input parameters for the specific case under analysis and to assess the uncertainty of the algorithm on diameters and lengths in relation to the cylindrical fitting procedure used. Finally, it is essential to assess how the presence of measurement noise on the point cloud affects dimensional measurements. Therefore, parameter sensitivity and Monte Carlo analyses, which are reported below, were carried out to tackle the issues.

4.1. Evaluation of optimal input parameters

The correct segmentation and reconstruction of the geometry is only possible after a careful choice of the algorithm's input parameters. The main ones to be provided to the TreeQSM algorithm are related to the initial process of partitioning the point cloud P into surface patches. This process reduces the computational complexity of the subsequent processing steps. Firstly, in order to determine the partition of the point cloud, points are randomly chosen, which will later be used as centres to define spherical domains, according to Equation (1):

$$\left|c_i - c_j\right| > d_{\min} \quad \forall c_i, c_j \in S \subset P, i \neq j\,, \tag{1}$$

where c_i, c_j belong to the point cloud P while S is the set of points chosen as centres. The diameter $d_{\min}$ is a fixed parameter defined by the user. A good rule of thumb is to initially set a diameter close to the mean value of the branch [21]. The partition is done by intersecting the spherical domains of diameter $d_{\min}$ with the point cloud P by the previously defined centre point c_i. In order to ensure that the number of central points is well distributed, the distance between any point and the central point is limited according to Equation (2):

$$\forall x \in P \quad \exists c_i \in S: |x - c_i| < d_{\min}. \tag{2}$$

In a second stage of the partition, the centre points are used to define spherical domains R_i of radius r_i that intersect the point cloud in the same way as in the first stage. The partition is defined in Equation (3) as follows:

$$\forall x \in P \quad R_i = \{x \in P: |x - c_i| < r_i\}\,. \tag{3}$$

In this case, the radius r_i, as opposed to the diameter $d_{\min}$ can assume a constant value or vary between a minimum $r_{\min}$ and a maximum $r_{\max}$ considering two consecutive surface patches generated by the intersection of P with two spherical domains of different radius, the number of points in common between the two is governed by the radius of the two spheres. Therefore, as this varies between $r_{\min}$ and $r_{\max}$, there will be a smaller or larger intersection between the surface patches.

In order to choose the appropriate values for these parameters in the specific case, an Artificial Point Cloud (APC) was created in the MATLAB environment, with dimensions of the same order of magnitude as the terminal branch under investigation. The geometry consists of 5 consecutive coaxial cylinders, as in Figure 7a. Their diameters are equal to d_{APC1} = 3.5 mm and d_{APC2} = 5 mm, respectively, while the overall height is h_{APC} = 132 mm. The latter values are chosen as representative of the branch diameters and lengths of the real fruit bearing shoot, accordingly to manual measurements reported in Figure 5b. The APC is built considering a random point distribution for each cylinder section of the artificial twig. The surface density, computed using the same procedure described in Section 2, is approximately 100 times less dense than the experimental point cloud. Therefore, the generated point cloud can be considered as a reference for accuracy estimation of the TreeQSM algorithm for the experimental case. The point cloud was processed by the TreeQSM algorithm as the parameters $r_{\min}$ and $r_{\max}$, varied, while the value of $d_{\min}$, was kept fixed at 3.5 mm, which is equal to the nominal diameter of the sprig. $r_{\min}$ was made to vary between 0.1 mm and 25 mm while $r_{\max}$ was made to vary between 2 mm and 25 mm, both with fixed steps of 0.1 mm. The optimal values of the parameters to obtain a good reconstruction of the artificial cloud were obtained by searching for the reconstruction that minimises the error between the estimated diameters and lengths compared to the nominal diameters and lengths set for the construction of the

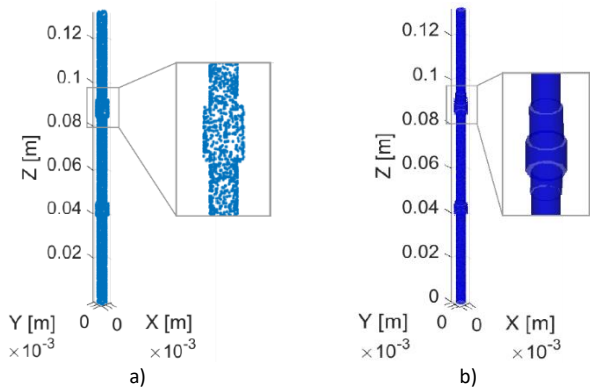

Figure 7. a) Artificial point cloud for choosing the optimal input parameters for the algorithm. b) Reconstruction of the cylindrical model with the optimal parameters for the TreeQSM algorithm.

Table 3. Comparison between the artificial point cloud and TreeQSM cylinder model with relative error percentage for the optimal parameters $r_{\min} = r_{\max} = 0.2$ mm.

	Artificial point cloud, mm	TreeQSM model, mm	Relative Error, %
d_{APC1}	3.50	3.54	1.14
d_{APC2}	5.00	4.91	1.80
h_{APC}	132.00	131.97	0.02

point cloud given as input to the TreeQSM algorithm. The value obtained is 0.2 mm for both $r_{\min}$ and $r_{\max}$ due to the regularity of the point cloud geometry. The reconstructed cylinder model with the optimal parameters is shown in Figure 7b. The comparison between dimensions relative to the APL and TreeQSM cylinder model with relative error percentage for optimal $r_{\min} = r_{\max} = 0.2$ mm is reported in Table 3. The relative error percentages are in the order of percentage point for the diameters and in the order of percentage point cents for the total twig height. The value of $r_{\min}$ and $r_{\max}$ are in line with the literature for the TreeQSM model [21].

4.2. Uncertainty estimation associated with measurement noise

Having known the optimal parameters for the purpose of reconstructing the cylindrical structure of the branch for the experimental case, it is of fundamental importance to assess how the measurement noise level in the point cloud reconstruction affects the identification of nodes and estimation of geometrical characteristics. Therefore, we investigate various levels of measurement noise in the point cloud provided as input to the TreeQSM algorithm, evaluating how they affect the reconstruction of the branch. Moreover, the acceptable maximum noise level allowed for a proper geometry reconstruction is pointed out. The noise on the point cloud depends on the quality of the images from which the cloud is reconstructed. This noise is due to the camera, the lens and, finally, the illumination that affects the contrast of the scene. To a first approximation, it can be regarded as a random distribution [22]. In addition, noise can result from the point cloud reconstruction due to misalignments and lack of clear references on the object surface, increasing the roughness of the reconstruction itself [23]. Again, it is possible to represent this effect with a random distribution.

To simulate the presence of noise, the geometry used to generate the input cloud for the algorithm was constructed with varying values of diameters and lengths according to a normal distribution with increasing standard deviation ranging from 0.001 mm to 1 mm, which is more than the order of node diameters to be identified. In this way, it was possible to simulate an increasing presence of noise which corresponds to a decreasing in the Signal-to-Noise Ratio (SNR), calculated as the ratio of the true size to the variability associated with the noise. The nominal point cloud is the one previously used for estimating the optimal input parameters. Diameters and heights remain unchanged. In particular, the lengths of the branch sections (corresponding to smaller diameters) are 4 cm while those of the two nodes are different, equal to 5 mm and 7 mm respectively. This is done in order to investigate the resolution of small geometric variations along the cloud axis as the artificially introduced noise changes. The APCs added with Gaussian noise are represented in Figure 8 with SNR indications on radius and height. The TreeQSM algorithm is used to reconstruct the branch structure using cylinders. As already pointed out, the presence of nodes is simulated by introducing two cylinders with a larger diameter than the rest of the model. These are then reconstructed by the algorithm with cylinders having a larger radius than the remaining parts. By evaluating the variation of the radius along the axis of the cylindrical model, it is possible to recognise the five different sections of the geometry by estimating their relative diameters and lengths. The variation of the radius along the axis of the cylindrical model is shown in Figure 9 as the SNR decreases. It is evident that as the SNR decreases, there is no longer a clear distinction between the larger and smaller diameter sections.

Figure 10 shows the values of the diameters and heights for the five identified model sections. As the SNR decreases, the algorithm can no longer recognise sections of different radius, i.e. nodes, as the effect of noise is preponderant. It is possible to identify nodes until a SNR value of 43.40 dB considering the nominal length and 5.85 dB with respect to the nominal radius. Consequently, the point density is lower for low SNRs in the graphs of Figure 10a and b. The 5 sections shown in the graphs relate to the 5 consecutive coaxial cylinders of which the initial geometry is formed: sections 1, 3 and 5 are related to the twig while sections 2 and 4 are the nodes.

4.3. Uncertainty on diameter and length estimation

Once the optimal initial parameters of the algorithm are defined and the weight of the measurement noise assessed, the ability of the algorithm to follow the shape variations, typical of the measurand, was investigated. Indeed, the presence of nodes is the main irregularity present in a branch. As introduced earlier, these were simulated using cylinders with a larger diameter than the rest of the model. Thus, it is possible to assess the uncertainty of the TreeQSM algorithm in estimating diameters and lengths.

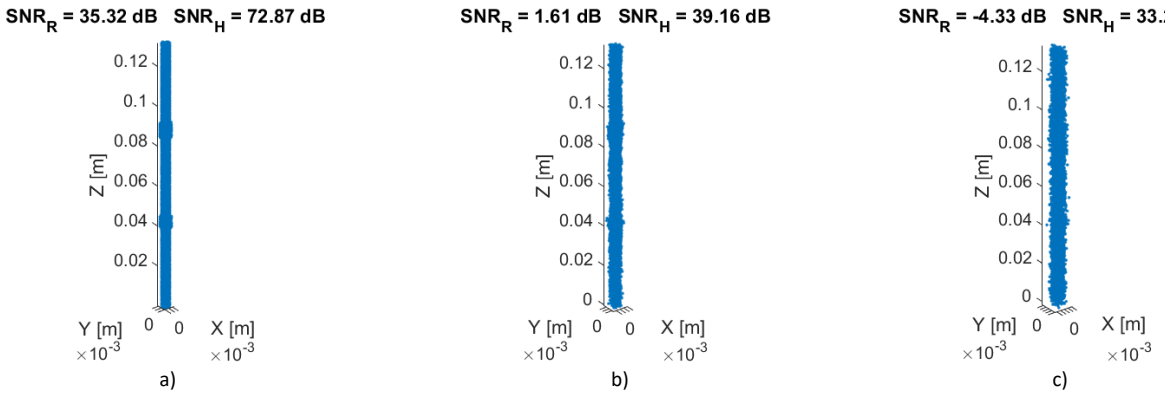

Figure 8. Point clouds for three increasing levels of noise.

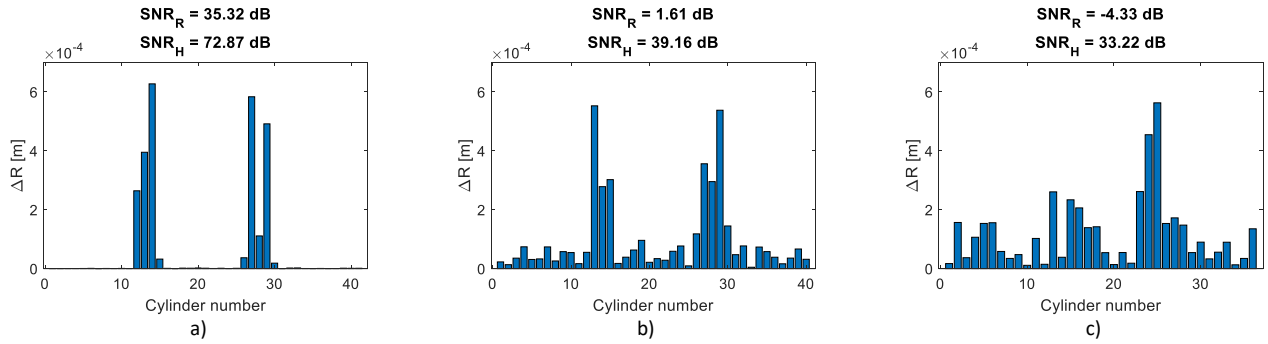

Figure 9. Variation of radius along the axis of the simulated branch for three increasing levels of noise.

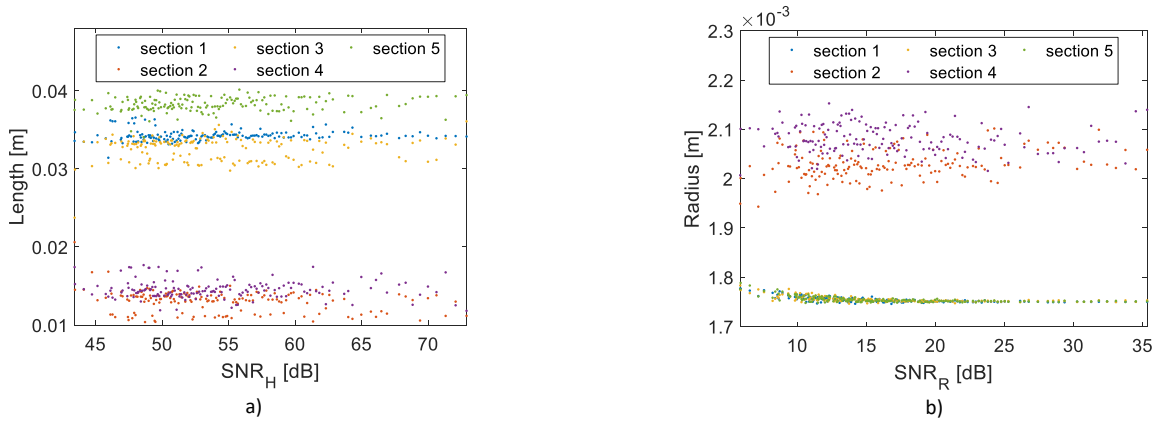

Figure 10. Estimation of a) the lengths and b) the radius of each section of the point cloud as the imposed Gaussian noise increases.

A Monte Carlo simulation was set up to obtain 100000 random point clouds by varying the length of the twig, its diameter and, finally, the diameter of the node according to a normal distribution representative of the real case scenario. In particular, once the diameter of the smallest cylinders, which represent the twig, is defined, the diameter of the largest cylinders, which simulate the presence of nodes, is chosen. The latter diameter has the value of the twig diameter as the minimum of the distribution, to avoid unrealistic conditions. The geometry used for the creation of the APCs is shown in Figure 11 along with the relevant dimensions. The characteristic dimensions of the twig geometry (h_r, h_n, d_r, d_n) are obtained considering a normal distribution with a coverage factor k of 2. The extremes of the distributions used for the generation of randomized APCs, which are shown in Table 4, are chosen consistently with the actual dimensions of the object under test and retrieved from the experimental data gathered manually with the use of a caliper.

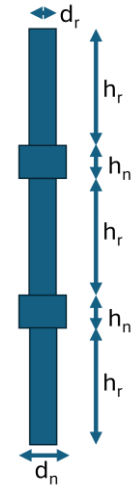

Figure 11. Geometry used to create the point cloud in estimating the measurement uncertainty of diameters (d) and lengths (h) using TreeQSM algorithm.

Each APC, having known nominal values, is given to the TreeQSM algorithm to obtain the cylinder model from which geometrical estimations are obtained. The latter are compared with the nominal values, evaluating the goodness of the algorithm for each specific iteration of the simulation.

Initially, the total height of the cylinder model, the minimum radius and the maximum radius were assessed. The deviations (i.e. the difference) between the nominal geometric parameters from the APCs built in MATLAB with respect to the same dimension estimated by TreeQSM algorithm are denoted by δ. The deviation of the quantity q is defined as in Equation (4):

$$\delta q = q_{\text{nominal}} - q_{\text{TreeQSM}}\,, \tag{4}$$

where $q = \{r_{\max}, r_{\min}, h_{\text{overall}}, h_r, h_n, r_r, r_n\}$. Outliers are removed using the Hampel identification algorithm. It consists of a median filter computed on a window composed of k samples

Table 4. Normal distribution parameters of the twig geometry for the Monte Carlo simulation.

	Mean value, mm	Standard deviation, mm	Description
d_r	3.50	0.25	Nominal diameter of the branch
d_n	5.00	0.25	Nominal diameter of the node
h_r	40.00	2.50	Nominal height of the branch
h_n	5.00	0.50	Nominal height of the node

Table 5. Mean deviation and relative standard deviations for the maximum radius, minimum radius and total height of the point cloud.

	Mean value, mm	Standard deviation, mm
$\delta r_{\max}$	0.07	0.07
$\delta r_{\min}$	0.00	0.03
$\delta h_{\text{overall}}$	0.90	4.26

centred around the target sample. The filter is only applied if the target sample differs from the window median by more than 3 standard deviations of the window [24]. Considering the distribution for each geometric parameter, TreeQSM algorithm mostly underestimates the nominal quantities. The $\delta r_{\max}$, $\delta r_{\min}$, $\delta h_{\text{overall}}$, δr_{r}, δr_{n}, δh_{r}, δh_{n} are respectively underestimated in the 98.82 %, 100 %, 94.43 %, 47.15 %, 100 %, 98.70 % and 0.40 % of the cases. Moreover, absolute values of the deviations are considered to compute mean and standard deviations. The only exception to the trend is the node length h_{n} which is mostly overestimated and characterized by a higher mean and standard deviation.

Table 5 shows the details relative to mean values and standard deviations of the geometrical deviations obtained on the 100000 APCs analysed in the Monte Carlo simulation. The mean value of the deviation indicates the accuracy of the algorithm in measuring the quantity in question while the standard deviation its precision.

The algorithm succeeds in estimating the nominal value of the minimum radius while the maximum radius is given with an accuracy of 0.07 mm. Moreover, it has a lower accuracy in estimating the total height which is approximately in the order of 1 mm. As pointed out in Section 4.2, it is possible to identify the five sections of which the starting point cloud is made up by exploiting the increase in diameter when nodes are present. To obtain this information, it is possible to evaluate the variation (i.e. the derivative) of the radius of the cylinders along the axis of the model reconstructed by TreeQSM. Nodes (i.e. larger cylinders) are identified if the variation in diameter between section is relevant. For our case, adjacent cylinders having at least a change in diameter of 0.04 mm are marked as nodes. This value is considered the minimum acceptable variation to have a node in the branch, and it is used only for computational identification purposes. Indeed, experimentally, the diameter variation is in the order of tenths of a millimetre. In the case of real branching, this derivative will be with respect to the curvilinear abscissa of the branching. The graph in Figure 12 is given as an example. The radii of the reconstructed model increase at the correspondence

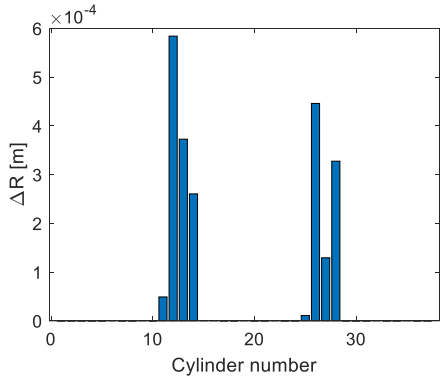

Figure 12. Difference between cylinder radii obtained via TreeQSM along the point cloud axis.

Table 6. Mean deviation and relative standard deviations for sections of the point cloud.

	Mean value, mm	Standard deviation, mm
δh_{r}	5.19	3.29
δh_{n}	7.83	1.67
δr_{r}	0.00	0.04
δr_{n}	0.38	0.21

of two intervals related to the presence of nodes. Using this information, it is possible to estimate the node position, length and radius of each section of the model.

As shown in Figure 11, in each artificial point cloud there are 3 equal sections corresponding to the twig, having diameter d_r and height h_{r}, and 2 equal sections corresponding to the nodes, having diameter d_{n} and height h_{n}. The deviations of the magnitudes for the branch and the node are then calculated. The mean values and standard deviations for the branch and the nodes are given in Table 6. The branch radius is well reconstructed reaching the nominal value while the node radius is characterised by an uncertainty approximately of 0.38 mm. The algorithm succeeds in reconstructing the diameter of longer cylindrical sections very accurately, where more data is available for the cylindrical fit, while it solves abrupt and short section changes in a worse way, however with tenth of a millimetre accuracy. When considering heights, these are reconstructed with errors in the millimetre range due to the difficulty in finding the correct sections boundaries in the geometry.

5. POINT CLOUD FEATURE EXTRACTION

After evaluating the uncertainty of the algorithm, the point cloud retrieved by the branch scan is processed using cylinder fitting to extract diameters along the curvilinear branch direction. The obtained cylinder model is shown in Figure 13. The cylinder diameters along the curvilinear main axis, which are highlighted in blue in the cylinder model, are reported in Figure 14a. The diameter naturally moves from bigger to smaller values, in the last section of the branch. This trend should be removed in order to evaluate the internode. Moreover, diameter peaks should be detected to evaluate the node diameters and internode behaviour along the principal axis. Therefore, the lower envelope of the cylinder diameter over the distance from the base is taken and used to calculate the proper branch average diameter, excluding the nodes. In this case, the average diameter for the principal axis is 2.14 mm along with a standard deviation of 0.90 mm, which completely falls within the experimental data represented in Figure 5 for the principal axis when nodes are not considered in the manual measurements. The envelope is depicted in red in Figure 14a while the detrended data, highlighting the diameter fluctuations, is shown in Figure 14b.

Nodes are then identified in the detrended data as diameter peaks. Node diameters over identified nodes, moving from the base to the branch end, are then represented in Figure 15a. It is clear that data follow a similar trend as the one represented in Figure 14a. In fact, nodes diameter reduces along the principal axis. The node average diameter and standard deviation for all the identified nodes in the present test case are respectively 2.94 mm and 1.20 mm. Moreover, the internode is computed as the difference between the position of adjacent nodes. Results are shown in Figure 15b. The internode average and standard deviation retrieved for all the identified nodes in the present test

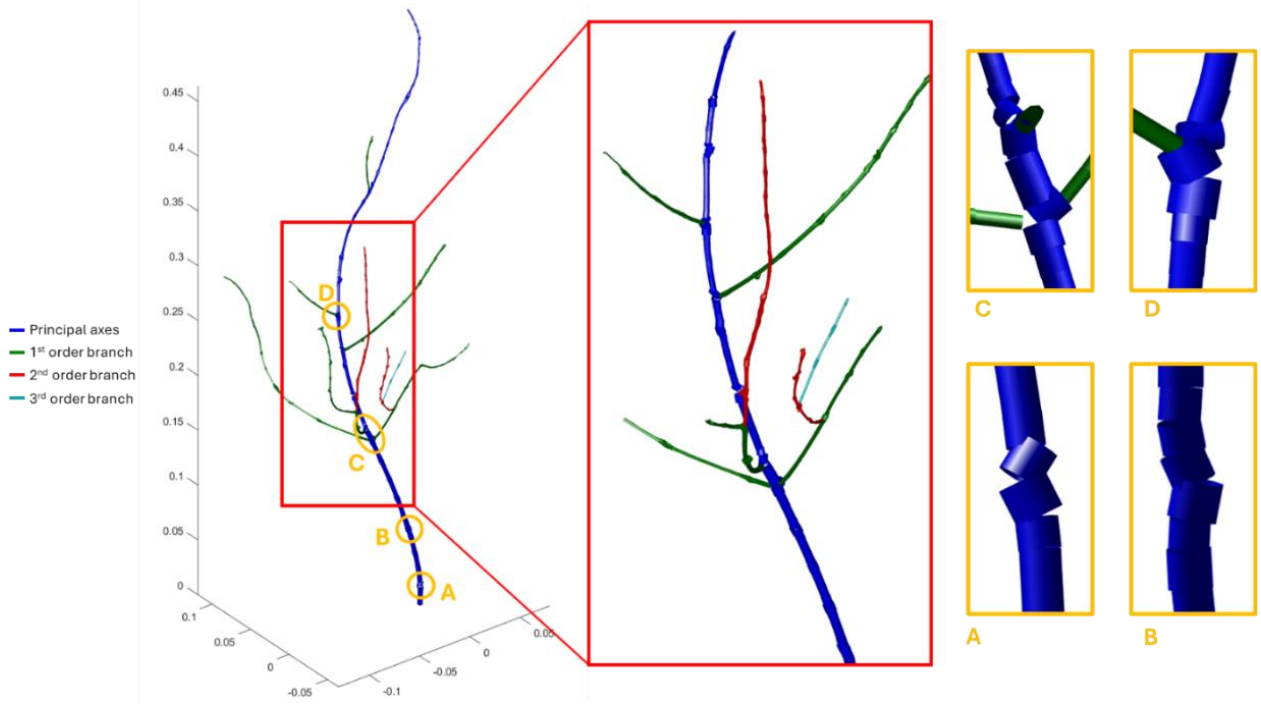

Figure 13. Cylinder fitting of the branch point cloud by TreeQSM. Examples of node reconstruction by cylinder fitting are highlighted in the yellow boxes.

case are respectively 14.38 mm and 7.78 mm. Data in Figure 15 is given with uncertainties found out in Section 4.3 as error bars.

The diameter along the principal axis and the diameter of the nodes result being compatible measurements. This is due to the nature of the fruit-bearing shoot under test, having older and younger sections respectively characterized by narrower and wider diameters. Therefore, the retrieved useful information from the presented procedure are the local diameter of the nodes and the internode, which are related to the local diameter of the branch.

Node diameter and internode fall within the specific variability of the fruit bearing shoot analysed and, therefore, can be considered as global indicators for the specific variety. The results shown are of fundamental importance as they make it possible to follow the progress and the variations of the node diameters and internodes along a specific branch axis, from older to younger section of the branch itself. Specifically, the internode is a typical indicator of the branch architecture between different olive varieties.

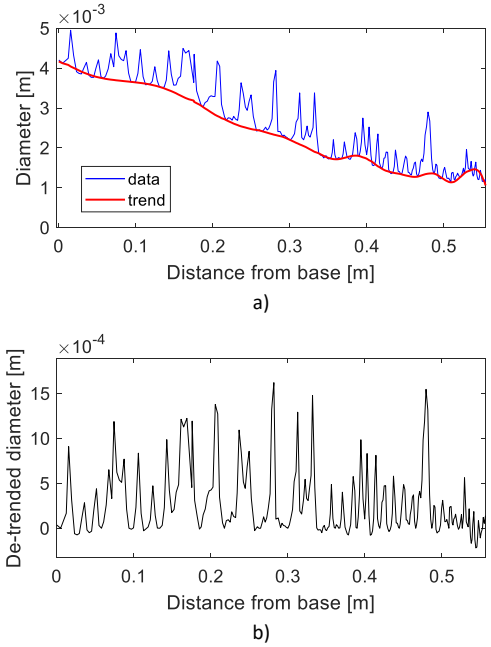

Figure 14. a) Cylinder diameter from the branch base along the principal axes and b) resulting detrended data, where only node diameter variation is highlighted.

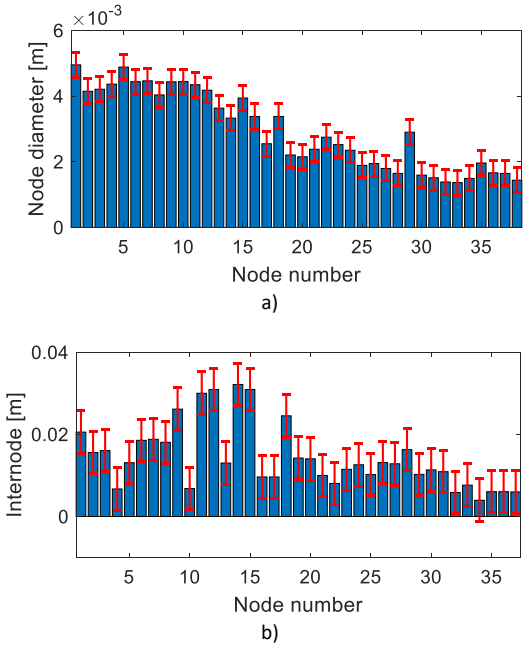

Figure 15. a) Node diameter over identified nodes; b) internode distance over identified nodes; uncertainties are given as red dots with a coverage factor $k = 2$.

6. CONCLUSIONS

Studying the tree architecture is fundamental in agronomic terms for the evaluation of the suitability of the olive varieties for the different planting systems and to properly manage the canopy through pruning. A new methodology for the optimal estimation of the diameter of branches of different order and degree is proposed, introducing the estimation of the internode, a parameter not investigated in the analysis algorithms to date. A sensitivity analysis was carried out on the input parameters to the TreeQSM algorithm by assessing the weight of measurement noise in the estimation of geometric quantities. It was found that the optimal values agree with those obtained in the literature. The analysis performed in the present study is pivotal since previous research only report data for tall trees, whereas no state-of-the-art studies dealing with olive trees were found. Therefore, verifying that the optimal parameters were congruent with the literature was a crucial result of this paper. Finally, an uncertainty on the estimation of diameters and lengths was provided by means of a Monte Carlo analysis. Considering the entire geometry, the maximum radius, coinciding with the nodes, is estimated with a 2σ uncertainty of 0.17 mm. Similarly, the uncertainty for the total height is 1.80 mm. APCs, created specifically for the aim of this study, are an approximation of the real case scenario. Indeed, APCs are characterized by a linear geometry and are made by simple geometrical elements. Nodes are modelled as abrupt geometrical changes in cylinder diameters and, lastly, misalignments or surface noise, present in the real case, are not being considered in the ideal case. Therefore, the accuracy in the evaluation of the twig diameter, characterized by the smaller value, is extremely low. This suggests a very accurate fitting of the cylinder model, which is a highly unlikely scenario due to the former motivations. However, the accuracy in the evaluation of the diameter's changes considering limited sections of the point cloud, modelling the presence of nodes. In fact, the algorithm must deal with the discontinuous change of the geometry, considered the worst-case scenario possible, and need to link the cylinder model properly to estimate the geometrical quantities.

Ultimately, the node locations are identified along the principal axis of the twig point cloud and, as a consequence, the average branch diameter, excluding nodes, is estimated to validate the proposed procedure comparing it with experimental data. The principal axis average diameter is 2.14 mm instead of 2.38 mm, obtained when considering nodes in the computation. Moreover, the node average diameter is 2.94 mm, and the average internode is 14.38 mm.

The present work is focused on the validation of the cylinder model approach used by TreeQSM for dimensional measurements and node identification in small branches and fruit bearing shoots. A systematic study of the uncertainty associated with the experimental setup, measurement repeatability and point cloud derivation (mainly caused by image alignment) will be taken into account in future works due to the number and the variability of parameters involved. The algorithm will be applied, verifying its performance, on a significative amount of point clouds obtained from olive tree branches with the aim to be used for the classification of different varieties according to their architectural characteristics.

AUTHORS' CONTRIBUTION

Alessandro Annessi: Conceptualization, Investigation, Data curation, Methodology, Formal analysis, Visualization, Writing – original draft;
Andrea Berdini: Investigation, Software;
Francesco Belluccini: Investigation, Conceptualization;
Matteo Zucchini: Conceptualization;
Veronica Giorgi: Supervision, Writing – review & editing;
Enrico Maria Lodolini: Conceptualization, Supervision, Writing – review & editing;
Milena Martarelli: Conceptualization, Methodology, Supervision;
Paolo Castellini: Funding acquisition, Resources, Supervision;
Davide Neri: Funding acquisition, Supervision

ACKNOWLEDGEMENT

The authors acknowledge founding from TeneRa of the operational group RiTA (ID 59750), "Valorization of genetic resources and introduction of innovative techniques for Ascolana tenera production" founded by PSR Marche 2014-2020 (16.1).

REFERENCES

[1] A. Larbi, M. Ayadi, A. Ben Dhiab, M. Msallem, J. M. Caballero, Olive cultivars suitability for high-density orchards, Spanish Journal of Agricultural Research, vol. 9 (2011) 4, pp. 1279–1286. DOI: 10.5424/sjar/20110904-062-11

[2] E. M. Lodolini, P. G. Lucchese, A. De Iudicibus, Canopy growth and architecture of five olive cultivars for high-density orchards, Acta Horticulturae (2023) 1366, pp. 275–282. DOI: 10.17660/ActaHortic.2023.1366.32

[3] J. Gonzalez de Tanago, A. Lau, H. Bartholomeus, M. Herold, V. Avitabile, P. Raumonen, C. Martius, R. C. Goodman, M. Disney, S.Manuri, A. Burt, K. Calders, Estimation of above-ground biomass of large tropical trees with terrestrial LiDAR, Methods in Ecology and Evolution, vol. 9 (2017) 2, pp. 223–234. DOI: 10.1111/2041-210x.12904

[4] E. M. Lodolini, E. Santilli, F. Zaffina, G. Toscano, S. Di Stefano, M. Naspi, A. Assirelli, Energetic Valorization of the Biomass from Olive Rejuvenation Pruning of Traditional Olive Orchards, Proc. of the 30th European Biomass Conf. and Exhibition, vol. 9-12 (2022), 5 pp. DOI: 10.5071/30THEUBCE2022-1DV.1.7

[5] G. Bucci, D. Bentivoglio, M. Belletti, A. Finco, Measuring a farm's profitability after adopting precision agriculture technologies: A case study from Italy, Acta IMEKO, vol. 9 (2020) 3, pp. 65-74. DOI: 10.21014/acta_imeko.v9i3.799

[6] L. M. Peppi, M. Zauli, L. Manfrini, L. Corelli Grappadelli, L. De Marchi, e P. A. Traverso, Low-cost, high-resolution and no-manning distributed sensing system for the continuous monitoring of fruit growth in precision farming, Acta IMEKO, vol. 12 (2023) 2, pp. 1–11. DOI: 10.21014/actaimeko.v12i2.1342

[7] S. Camposeo, G. Ferrara, M. Palasciano, A. Godini, Varietal behaviour according to the superintensive oliveculture training system, Acta Horticulturae (2008) 791, pp. 271–274. DOI: 10.17660/actahortic.2008.791.38

[8] A. Rosati, A. Paoletti, S. Caporali, E. Perri, The role of tree architecture in super high density olive orchards, Scientia Horticulturae, vol. 161 (2013), pp. 24–29. DOI: 10.1016/j.scienta.2013.06.044

[9] A. Carella, R. Massenti, G. Milazzo, T. Caruso, R. Lo Bianco, Fruiting, Morphology, and Architecture of 'Arbequina' and 'Calatina' Olive Branches, Horticulturae, vol. 8 (2022) 2, p. 109. DOI: 10.3390/horticulturae8020109

[10] Y. Lin, S. Filin, R. Billen, N. Mizoue, Co-developing an international TLS network for the 3D ecological understanding of global trees: System architecture, remote sensing models, and functional prospects, Environmental Science and Ecotechnology, vol. 16 (2023), p. 100257.
DOI: 10.1016/j.ese.2023.100257

[11] W. Yang, P. Wilkes, M. B. Vicari, K. Hand, K. Calders, M. Disney, Treegraph: tree architecture from terrestrial laser scanning point clouds, Remote Sens Ecol Conserv, vol. 10 (2024) 6, pp. 755–774.
DOI: 10.1002/rse2.399

[12] M. Åkerblom, P. Raumonen, R. Mäkipää, M. Kaasalainen, Automatic tree species recognition with quantitative structure models, Remote Sensing of Environment, vol. 191 (2017), pp. 1–12.
DOI: https://doi.org/10.1016/j.rse.2016.12.002

[13] F. Fiorillo, C. Rossi, 3D survey and metric analysis of the Late Roman Fort of Umm al-Dabadib (Egypt), Acta IMEKO, vol. 7 (2018) 3, pp. 57-63.
DOI: 10.21014/acta_imeko.v7i3.590

[14] C. Marín-Buzón, A. M. Pérez-Romero, M. J. León-Bonillo, R. Martínez-Álvarez, J. C. Mejías-García, F. Manzano-Agugliaro, Photogrammetry (SfM) vs. Terrestrial Laser Scanning (TLS) for Archaeological Excavations: Mosaic of Cantillana (Spain) as a Case Study, Applied Sciences, vol. 11 (2021) 24, p. 11994.
DOI: 10.3390/app112411994

[15] A. Dietmaier, G. J. McDermid, M. M. Rahman, J. Linke, R. Ludwig, Comparison of LiDAR and Digital Aerial Photogrammetry for Characterizing Canopy Openings in the Boreal Forest of Northern Alberta, Remote Sensing, vol. 11 (2019) 16, p. 1919.
DOI: 10.3390/rs11161919

[16] S. R. Rogers, I. Manning, W. Livingstone, Comparing the Spatial Accuracy of Digital Surface Models from Four Unoccupied Aerial Systems: Photogrammetry Versus LiDAR, Remote Sensing, vol. 12 (2020) 17, p. 2806.
DOI: 10.3390/rs12172806

[17] S. Catalucci, R. Marsili, M. Moretti, G. Rossi, Point cloud processing techniques and image analysis comparisons for boat shapes measurements, Acta IMEKO, vol. 7 (2018) 2, pp. 39-44.
DOI: 10.21014/acta_imeko.v7i2.543

[18] N. Covre, A. Luchetti, M. Lancini, S. Pasinetti, E. Bertolazzi, M. De Cecco, Monte Carlo-based 3D surface point cloud volume estimation by exploding local cubes faces, Acta IMEKO, vol. 11 (2022) 2, pp. 1-9.
DOI: 10.21014/acta_imeko.v11i2.1206

[19] M. Akerblom, P. Raumonen, M. Kaasalainen, S. Kaasalainen, H. Kaartinen, Comprehensive quantitative tree models from TLS data, Proc. of the IEEE Int. Geoscience and Remote Sensing Symp., Munich, Germany, 22-27 July 2012.
DOI: 10.1109/igarss.2012.6352751

[20] P. Raumonen, M. Kaasalainen, M. Åkerblom, S. Kaasalainen, H. Kaartinen, M. Vastaranta, M. Holopainen, M. Disney, P. Lewis, Fast Automatic Precision Tree Models from Terrestrial Laser Scanner Data, Remote Sensing, vol. 5 (2013) 2, pp. 491–520.
DOI: 10.3390/rs5020491

[21] M. Åkerblom, Quantitative tree modeling from laser scanning data, Master's Thesis, Tampere University of Technology, 2012.

[22] J. Owotogbe, T. Ibiyemi, B. Adu, A comprehensive review on various types of noise in image processing, Int. Journal of Scientific & Engineering Research, vol. 10 (2019) 11, pp. 388–393. Online [Accessed 18 June 2025]
https://www.researchgate.net/publication/338112901

[23] I. Nikolov, C. Madsen, Rough or Noisy? Metrics for Noise Estimation in SfM Reconstructions, Sensors, vol. 20 (2020) 19, p. 5725.
DOI: 10.3390/s20195725

[24] R. K. Pearson, Y. Neuvo, J. Astola, M. Gabbouj, Generalized Hampel Filters, EURASIP J. Adv. Signal Process, (2016) 87, 18 pp.
DOI: 10.1186/s13634-016-0383-6